Early stage electromigration in gold thin films

S. Bai and K. P. Roenker

Citation: Journal of Applied Physics **84**, 4248 (1998); doi: 10.1063/1.368641
View online: http://dx.doi.org/10.1063/1.368641
View Table of Contents: http://scitation.aip.org/content/aip/journal/jap/84/8?ver=pdfcov
Published by the AIP Publishing

Early stage electromigration in gold thin films

S. Bai and K. P. Roenker[a)]
Department of Electrical and Computer Engineering and Computer Science, University of Cincinnati, Cincinnati, Ohio 45221-0030

(Received 27 April 1998; accepted for publication 20 July 1998)

The early stage of electromigration in thin gold films on polyimide has been investigated at room temperature using the resistometric technique. While the resistance increase is initially linear, a saturation tendency is observed for longer stressing times at all stress current densities. A simple model is described which relates the saturation behavior in the resistance change to the buildup of mechanical stress gradients, which produce a counterflux of metal ions proportional to the stress gradient. The stress gradients arise due to nonuniformity in the grain size in the polycrystalline thin metal films which produces cluster regions of small grain size alternating with regions of large or near-bamboo grain size, which have larger and smaller metal ion diffusivities, respectively. The dependence of the maximum level of the resistance's change and the rate of resistance increase on the stress current density are experimentally characterized and compared with the model's predictions with good agreement. © *1998 American Institute of Physics.* [S0021-8979(98)07320-4]

I. INTRODUCTION

Gold and multi-component, gold-based metal systems are widely used for metallic connections to III–V-based electronic and optoelectronic semiconductor devices. For some devices, such as semiconductor lasers and metal-semiconductor field effect transistors (MESFETs) and heterojunction bipolar transistors (HBTs) for high power applications, current densities in the thin film metal connections can reach 10^6 A/cm^2, which can produce electromigration (EM) concerns.[1–5] Self-heating in the semiconductor devices and joule heating in the metal can also produce elevated temperatures that accelerate the EM phenomenon.[6] In addition, tensile stresses can arise in metal interconnects during fabrication due to the elevated deposition temperature and the mismatch between the metal and substrate's thermal expansion coefficients. Such tensile stresses can create voids which can significantly enhance EM damage.[7–9] The problem of electromigration in gold-based metallization systems has been previously investigated,[10–21] but has been reexamined here in the light of recent progress in understanding the phenomenon in aluminum-based metallization and because of the growing commercial interest in III–V electronic and optoelectronic semiconductor devices and integrated circuits.

In this work the early stage of electromigration in thin gold films has been investigated using the resistometric technique where the change in resistance in long, thin metal resistors is monitored as a function of electrical stress time.[11,13,22,23] The study of the early stages of electromigration is of interest for understanding the fundamental physical mechanisms underlying the phenomenon since the current density is more nearly uniform throughout the thin film and the effects of electrical stress are not evolving as rapidly as near failure. In addition, the study of early resistance changes is relevant since a rapid, initial rate of resistance change has been found to correspond to a short mean time to failure.[14,22] For thin metal films, the study of resistance change is useful in investigating electromigration because the resistance is a function of the film's polycrystalline structure and is sensitive to the formation of voids at grain boundaries whose growth can eventually lead to line failure.[23,24] The thin film's initial polycrystalline structure and resistance are known to be a function of the deposition conditions and sample's thermal history.[25] To date, the study of EM induced early resistance change has usually described a linear rate of resistance variation.[10,11] In this work we report results of an investigation of early changes in resistance in thin gold films where the resistance increase shows a clear saturation effect that has not been described or explained in detail in previous reports. In the following section we describe a simple model to explain the saturation effect which is based on the formation of mechanical stress gradients within the small grain, polycrystalline line segments, or grain cluster regions following the description of Korhonen *et al.*[9,26] and Knowlton *et al.*[24] These stress gradients increase with increasing EM transport and result in a counter flux of ions driven by the stress gradient. As the EM proceeds, the resistance initially increases due to the formation of voids induced by the EM, but eventually shows a saturation tendency when the ion flux due to EM is nearly counterbalanced by the flux driven by the mechanical stress gradient. Subsequently, we present experimental results from EM studies in thin gold films which illustrate the described effects. In the final section we summarize our results and draw conclusions with regards to the use of early resistance studies for investigating the EM phenomenon.

II. MODEL FOR TIME DEPENDENT RESISTANCE CHANGE

For modern interconnects between devices, the linewidth can approach the metal grain size so that the microstructure of the metal line can consist of regions of large and small

a)Electronic mail: kroenker@ececs.uc.edu

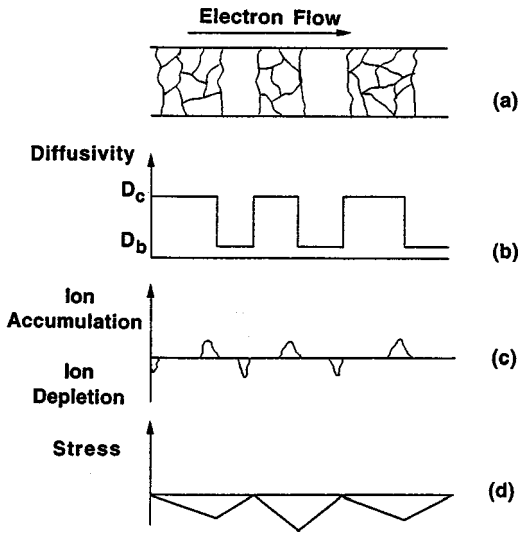

FIG. 1. (a) Microstructure of metal line consisting of small grain clusters and large grain (bamboo or near-bamboo) regions. (b) Associated atomic diffusivities in cluster D_c and near-bamboo regions D_b, respectively. (c) Electromigration induced ion accumulation and depletion. (d) Mechanical stress profile in cluster and near-bamboo regions.

grain size as shown in Fig. 1(a). When the linewidth becomes sufficiently small, an individual grain can become large enough to span the linewidth, in which case it is described as a bamboo grain. For this discussion, we will describe the microstructure regions of large and small grain size of a metal line as bamboo or near bamboo and polygranular cluster or, simply cluster regions, respectively.[9,24] The microstructure of the metal interconnects is of importance because the effects of electromigration are dependent upon the grain structure and its uniformity.[9,12,24,26] EM arises due to atomic diffusion of metal ions which occurs primarily along grain boundaries in polycrystalline metal films.[12] The atomic flux is larger in cluster regions than the near-bamboo regions because of the larger density of grain boundaries and the lower atomic diffusivity within grains. Knowlton *et al.*[24] define separate and different effective atomic diffusivities for the two regions, i.e., D_b within bamboo grains and D_c in cluster regions as seen in Fig. 1(b).

When an EM inducing stress current is applied, the atomic flux density J at any point is given by[9,24,26]

$$J=\frac{D}{k_BT}\left\{\frac{d\sigma}{dx}+\gamma\right\}, \tag{1}$$

where D is the effective atomic diffusivity, T is the absolute temperature, σ is the mechanical stress, and γ is the EM driving force defined by qZ^*E/Ω where E is the electric field, Z^* is the effective charge on the diffusing ion, q is the magnitude of the electronic charge, and Ω is the atomic volume. At the outset of electrical stressing, the initial ion flux is due to EM only. In this case Eq. (1) gives the usual EM result of ion transport producing void formation and growth, and an increase in the metal line resistance. However, prior to EM stressing, there may be an initial tensile mechanical stress in the metal thin film due to the high temperatures employed in metal deposition and the difference in the thermal expansion coefficients between the substrate and metal film. The presence of this stress can give rise to voids, which can contribute to EM damage.[27] However, as the EM proceeds, due to more rapid ion transport in the cluster regions, a depletion occurs at the upstream side of electron flow (cathode end) and accumulation at the downstream side (anode end) of the cluster regions of small grains as shown in Fig. 1(c).[9,24,26] This material transport gives rise to an oscillating mechanical stress gradient along the cluster and near-bamboo regions as shown in Fig. 1(d).[9,24,26,27] As described by Korhonen *et al.*,[9,26] the rate of stress formation is given by

$$\frac{\partial\sigma}{\partial t}=\frac{\partial}{\partial x}\left[\kappa\left(\frac{d\sigma}{dx}+\gamma\right)\right], \tag{2}$$

where κ is the effective diffusivity defined by $\kappa=DB\Omega/k_BT$ where B is the effective bulk modulus. For a constant electrical stress and a finite length L (taken here to be the cluster length), Korhonen *et al.*[26] have shown that the solution for the time dependent stress buildup is given by

$$\sigma(x,t)=\gamma L\left[\frac{1}{2}-\frac{x}{L}-4\sum_{n=0}^{\infty}\frac{\cos\left[(2n+1)\pi\frac{x}{L}\right]}{(2n+1)^2\pi^2}\times\exp\left\{\frac{-(2n+1)^2\pi^2\kappa t}{L^2}\right\}\right]. \tag{3}$$

This result describes the formation of a stress distribution along the cluster region that saturates in a final linear form given by

$$\sigma(x,t\to\infty)=\gamma L\left[-\frac{1x}{2L}\right]. \tag{4}$$

This corresponds to tensile stress at the cathode end and compressive stress at the anode end of the cluster regions.

From Eq. (3) we can get the following expression for the time and spatial dependence of the stress gradient in the cluster region:

$$\frac{d\sigma}{dx}(x,t)=-\gamma\left[1-4\sum_{n=0}^{\infty}\frac{\sin\left[(2n+1)\pi\frac{x}{L}\right]}{(2n+1)\pi}\times\exp\left\{\frac{-(2n+1)^2\pi^2\kappa t}{L^2}\right\}\right]. \tag{5}$$

Since the higher order terms die out more quickly and are smaller in magnitude, we keep for simplicity only the first term in the sum so that as a first approximation we get

$$\frac{d\sigma}{dx}(x,t)\approx-\gamma\left[1-\frac{4}{\pi}\sin\left(\frac{\pi x}{L}\right)\exp\left\{\frac{-\pi^2\kappa t}{L^2}\right\}\right], \tag{6}$$

which gives a stress gradient buildup that saturates exponentially with time. When there is an initial tensile stress in the metal film due to fabrication, the stress causes void forma-

tion which modifies the above described results somewhat, but does not change the characteristic time dependence.[9,26] Since the voids are effective sinks and sources for the atoms, the stress must go to zero at such sites. As a result, the presence of voids at the cathode ends of the cluster regions causes the stress distribution to shift to a compressive nature all along the cluster length, but to retain its original spatial dependence.[9,26] The stress distribution in this case is shown in Fig. 1(d). The presence of an initial tensile stress due to fabrication modifies the initial but not the final spatial dependence of the stress.[9]

While the stress gradient given in Eq. (6) shows a nonuniform distribution along the cluster length, we will employ the result at the midpoint of the cluster, i.e., $x=L/2$, given in Eq. (7) below

$$\frac{d\sigma}{dx}\left(\frac{L}{2},t\right)\approx-\gamma\left[1-\frac{4}{\pi}\exp\left\{\frac{-\pi^2\kappa t}{L^2}\right\}\right] \tag{7}$$

because it emphasizes the exponential time dependence, which is important in understanding the behavior seen in the EM induced resistance changes reported here. Substituting Eq. (7) back into Eq. (1) we get the following simple but characteristic result for the time dependence of the net ion flux density (EM minus the mechanical stress gradient induced):

$$J(t)=\frac{4D\gamma}{\pi k_B T}\exp\left\{\frac{-\pi^2\kappa t}{L^2}\right\}=J_0 e^{-\alpha t}. \tag{8}$$

This result says that the net ionic flux density decreases exponentially with a rate constant α given by

$$\alpha=\frac{\pi^2\kappa}{L^2}=\frac{\pi^2 BD\Omega}{k_B T L^2}, \tag{9}$$

where we have substituted for κ from its definition above. From Eq. (8), the initial value of the ion flux density is that due to EM alone and is given by

$$J_0=\frac{4}{\pi}\frac{DqZ^*\rho}{\Omega k_B T}\,j, \tag{10}$$

where we have substituted for γ from above and used $E=\rho j$ where E is the applied electric field, ρ is the electrical resistivity of the metal, and j is the electrical current density. Aside from the prefactor $4/\pi$, which is of the order of one, this is the usual expression for the ion flux due to EM.[11]

We can now obtain an expression for the rate of resistance change for our metal interconnect using Eq. (8). Starting from $R=\rho L_m/A$, where L_m is the metal line length and A is the cross-sectional area, we get the rate of resistance change related to the change in cross-sectional area

$$\frac{1}{R_0}\frac{dR(t)}{dt}=\frac{-1}{A_0}\frac{dA(t)}{dt}, \tag{11}$$

where R_0 is the initial line resistance and we have assumed that the thin film's electrical resistivity is unchanged. Following Tang *et al.*,[10] we assume EM forms cylindrical voids of radius r equal in height to the line thickness h so that the cross-sectional area of the metal line is given by $A(t)=A_0-2hr(t)$ and the rate of change of the cross-sectional area is given by

$$\frac{dA(t)}{dt}=-2h\,\frac{dr(t)}{dt}. \tag{12}$$

The rate of increase of the void radius dr/dt is then related to the rate of ion depletion dn/dt by

$$\frac{dn(t)}{dt}=2\pi Nhr\,\frac{dr(t)}{dt}. \tag{13}$$

Combining the results in Eqs. (12) and (13) we get

$$\frac{dA(t)}{dt}=\frac{-1}{\pi Nr}\frac{dn(t)}{dt} \tag{14}$$

and substituting this result in Eq. (11) gives for the rate of resistance change

$$\frac{1}{R_0}\frac{dR(t)}{dt}=\frac{1}{\pi NrA_0}\frac{dn(t)}{dt}. \tag{15}$$

Finally, we can relate the rate of ion depletion dn/dt to the net ion flux $J(t)$ using

$$\frac{1}{A_0}\frac{dn(t)}{dt}=J(t)=J_e-J_\sigma(t), \tag{16}$$

where J_e is the EM flux and J_σ is the stress gradient flux. Then, substituting for $J(t)$ from Eq. (8) and substituting Eq. (16) into Eq. (15) we get

$$\frac{1}{R_0}\frac{dR(t)}{dt}=\frac{1}{\pi Nr}\,J(t)=\frac{J_0}{\pi Nr}\,e^{-\alpha t}. \tag{17}$$

Defining the saturation parameter C as

$$C=\frac{J_0}{\pi Nr\alpha}=\frac{4}{\pi^4}\frac{qZ^*L^2\rho}{rB\Omega}\,j \tag{18}$$

then the expression for the rate of resistance change Eq. (17) becomes

$$\frac{1}{R_0}\frac{dR(t)}{dt}=\alpha Ce^{-\alpha t} \tag{19}$$

and we can integrate and rewrite to obtain the final result

$$\frac{\Delta R(t)}{R_0}=\frac{R(t)-R_0}{R_0}=C(1-e^{-\alpha t}). \tag{20}$$

This result suggests that we can expect an initial linear increase in line resistance due to EM induced void formation, but also a saturation effect as the EM ion transport and deposition causes a mechanical stress gradient to form in cluster regions which produces a counterflux of ions that grows and eventually matches that due to EM. This will be the case as long as the length of the cluster region is shorter than some critical length L_c where the void growth reaches sufficient size so that line failure occurs.[26] From Eq. (20) we see that the saturation value of the resistance change ΔR is given by the parameter C and that in this simple model it is expected to be linearly dependent on the electrical stress current density j [see Eq. (18)]. This is not surprising since the

initial ion flux J_0 due to EM is also proportional to j as seen in Eq. (10). Finally, the resistance change saturates when the ion counter flux due to the mechanical stress gradient matches that due to EM. From Eq. (2) this occurs when

$$\frac{d\sigma}{dx}(x,t\rightarrow\infty)=-\gamma, \tag{21}$$

which is also what we obtain from Eqs. (5) and (6) when $t \rightarrow \infty$.

As defined earlier, the time dependence of the resistance change given in Eq. (20) is characterized by the parameter α. To lowest order, the rate constant α given by Eq. (9) is independent of the stress current density j. However, α is proportional to the effective atomic diffusivity D which is known to be an exponentially increasing function of the mechanical stress σ,[24] so the simple expression given in Eq. (9) is only a first order approximation for α.

The result given in Eq. (20) differs from the usual time dependence quoted for the resistance change given as[11]

$$\frac{\Delta R(t)}{R_0}=A^* j^n t e^{-Q/k_B T}, \tag{22}$$

where Q is the activation energy of electromigration, A^* is a constant dependent on the film geometry, and n is the exponent of the current density j which is typically between 1 and 3. For comparison with our result, we can rewrite Eq. (20) for short times ($\alpha t \ll 1$) to show the initial linear time dependence

$$\frac{\Delta R(t)}{R_0}\approx \alpha C t. \tag{23}$$

From our model, the prefactor αC can be found from substituting Eqs. (9) and (19) to give

$$\alpha C=\frac{4}{\pi^2}\left(\frac{qZ^*D\rho}{rk_BT}\right)j. \tag{24}$$

This result gives a linear dependence on the current density j which is somewhat different from the nth power seen in Eq. (22), though n is sometimes reported as unity.[11] The result in Eq. (24) also gives the linear dependence on the effective diffusion constant D which gives the usual exponential dependence on the activation energy seen in Eq. (22).

A nonlinear time dependence in the resistance change has been previously reported by several authors.[17,28,29] Scorzoni *et al.*[28,29] reported a nonlinear resistance change in EM stressing in Al/Si thin films which fit a square root of time dependence. They attributed the nonlinear time dependence to the formation of an oscillating pattern in the mechanical stress in the metal line due to the presence of alternating bamboo grains and small grain clusters. Li *et al.*[23] reported resistance changes in EM stressing in Al/Si thin films which showed a saturating behavior which they described but did not analyze. They also attributed the saturation effect to the formation of mechanical stress gradients in the metal line.

In the following section we provide experimental results for EM in gold thin films which demonstrate the saturation behavior in the resistance change described above. The dependence of the α and C parameters on the current density j is experimentally examined and compared with that predicted by the above described simple model.

III. EXPERIMENTAL RESULTS

Electromigration test structures were designed following Schafft[30] with line lengths $L_m=400$, 600, and 800 μm and linewidths $W_m=2$, 4, and 5 μm. The test line was connected at each end by an end-contact segment of width W_s and length L_s where W_s was set equal to 2 W_m and length L_s was set at 120 μm. For the voltage taps at the end of the test lines, the tap linewidth was set equal to W_m and the length set at 130 μm. The metal test structures were fabricated on 400 nm thick polyimide spin coated on silicon substrates. Gold was deposited using e-beam evaporation and the test structures were defined using standard photolithographic lift-off techniques. The EM stressed portions of the test structures were fabricated with 80 nm gold while the end contact pads were covered with a second metallization (Ti/Pt/Au) to a thickness of 500 nm for reliability during probing.

Constant current electrical stressing was employed using a Keithley Model 220 programmable dc current source operated in combination with a Hewlett-Packard Model 3478 multimeter in order to more precisely control the magnitude of the stressing current. Test voltages were measured using a Keithley Model 192 programmable digital multimeter. The test samples were probed using a micromanipulator Model 6000 probe station and all measurements were performed at room temperature. Only dc stressing was investigated in this work. For EM stressing, the electrical current densities employed in this study ranged from 1×10^6 to 1.2×10^7 A/cm^2. At interruptions in the stressing, resistance measurements were performed at a much lower current density, e.g., 1×10^5 A/cm^2, which was sufficiently low to avoid EM. The resistance changes measured were found to be stable. That is, no significant decay of the resistance changes was seen when monitored after EM stressing, which indicates that joule heating effects were not responsible for the observed resistance changes.

Shown in Fig. 2 are characteristic resistance changes (normalized to the initial resistance) seen as a function of stress time for a series of electrical current densities from 10^6 to 10^7 A/cm^2. While the resistance increase is linear at short times, there is a clear saturation tendency in each case such as that predicted in the analysis described above. Also apparent in Fig. 2 is that the saturation level of the resistance change increases with increasing electrical stress current density, which was also predicted. To compare these results with the model, the saturation value C was extracted from the resistance variations; the results are shown in Fig. 3 as a function of the stress current density j. The saturation parameter C shows a clear rise with current density. However, from Eq. (18) the model predicts a simple linear dependence on the current density while the experimental results suggest a $j^{1.5}$ dependence. The added dependence seen here on the current density may arise from the dependence of the effective atomic diffusivity D on the mechanical stress σ as de-

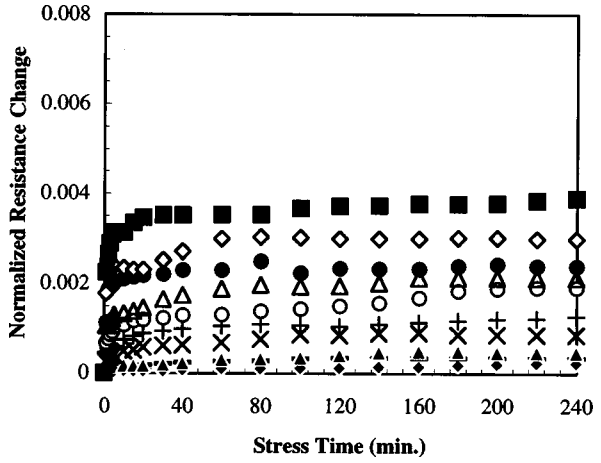

FIG. 2. Normalized resistance changes at room temperature vs stress time for various EM stress current densities starting at 1×10^6 A/cm^2 in increments of 1×10^6 A/cm^2 for an 80 nm thick gold metal line of 800 μm length and 4 μm width.

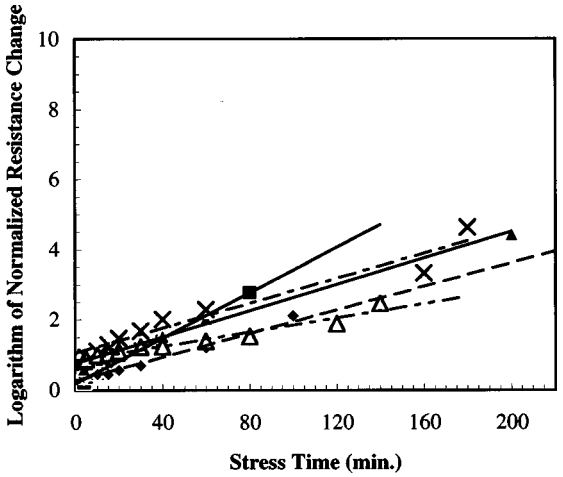

FIG. 4. Logarithm of resistance change [described in Eq. (27)] vs stress time for various EM stress current densities starting at 2×10^6 A/cm^2 in increments of 1×10^6 A/cm^2.

scribed above and reported by Knowlton *et al.*,[24] but further study is needed to clarify this.

Using the expression derived above for C given in Eq. (18), we can estimate the magnitude of the dependence of C on the electrical stress current density j predicted by our model. Using the following parameters for gold:[13,31–34] $Z^*=10$, $\rho=2.25\times10^{-8}$ Ω m, $B=7.45\times10^{10}$ N/m^2, and $\Omega=1\times10^{-29}$ m^3, we obtain

$$C=2\times10^{-9}\left(\frac{L^2}{r}\right)j. \tag{25}$$

Assuming a cluster length $L=2$ μm and a void radius of $r=0.1$ μm, then we get for C the result

$$C=8\times10^{-4}j\left(\frac{10^6\ \text{A}}{\text{cm}^2}\right), \tag{26}$$

where j is expressed in units of 10^6 A/cm^2. This result gives a value of 8×10^{-3} at $j=10^7$ A/cm^2, which is the same order of magnitude seen in Fig. 2 (4×10^{-3}) at this current density. Closer agreement with the experimental results may not be possible since we have obtained Eq. (26) based on estimates of the cluster length and initial void radius which are not well known. The important result here is that the model provides a description of the observed temporal behavior and a reasonable estimate of the magnitude of the resistance change described by the prefactor in Eq. (26).

To further compare the experimental results with the model, the resistance data were replotted as seen in Fig. 4 to determine the rate constant α. Rearranging Eq. (20) we get

$$-\ln\left[1-\frac{\Delta R(t)}{R_0}\right]=\alpha t \tag{27}$$

so that a plot of the quantity on the left hand side of Eq. (27) versus time is expected to yield a linear plot with a slope equal to the parameter α. As can be seen in Fig. 4, the form of Eq. (27) provides a reasonable description of the experimental results at each current density. When the rate parameter α was extracted from the slope for each current density, the results are seen in Fig. 5. The expression derived in our model and given by Eq. (9) predicts an α that is independent of the current density j to lowest order. Using the parameters for gold given above and the diffusion constants for gold

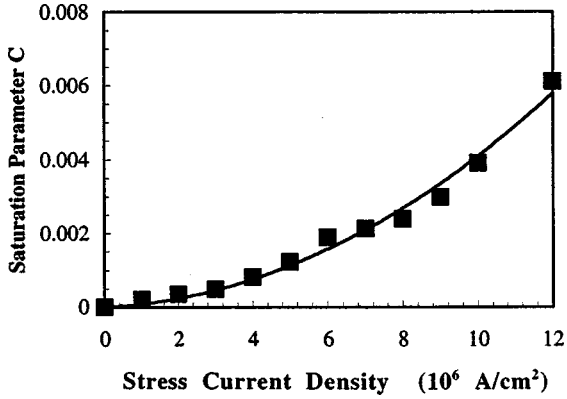

FIG. 3. Measured saturation parameter C (♦) vs EM stress current density j from the results in Fig. 2. Also shown (solid line) is the fit to the data given by the expression $C(j)=1.2\times10^{-4}(j/10^6\ \text{A/cm}^2)^{1.5}$.

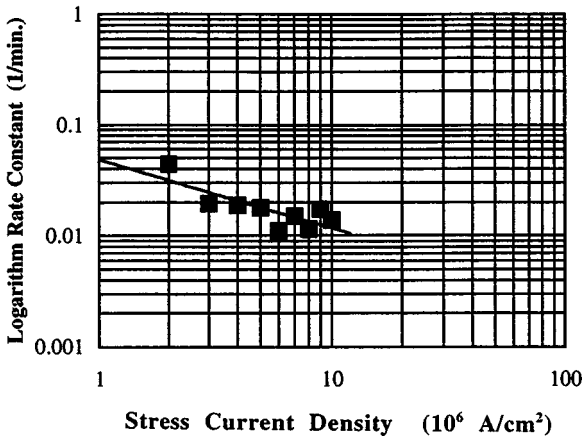

FIG. 5. Electromigration rate constant α as a function of the EM stress current density.

in thin films,[2,10,13] namely $Q=0.90$ eV and $D_0=5.3\times10^{-7}$ m^2/s, we calculate a value for the diffusion constant D at room temperature of 2.9×10^{-22} m^2/s and a value of α of 7.7×10^{-6}/min. This is a factor of 10^3 smaller than the magnitude seen in Fig. 4 $(1-4\times10^{-2}$/min). However, the diffusion constant is known to be enhanced by the presence of mechanical stress.[35] Following the analysis of Kinsbron *et al.*, we calculate an enhanced diffusion constant D' related to the original D by

$$D' = \frac{Y\Omega}{2k_BT(1-\nu)}\,D, \tag{28}$$

where Y is Young's modulus ($\approx B$) and the other parameters have been defined previously. Evaluating Eq. (28) using the parameters for gold we find that the diffusion constant is enlarged by a factor of 157 by the mechanical stress so that α is increased to 1.2×10^{-3}/min. This is still a factor of 10 less than that seen experimentally. However, neglected in the above analysis is any temperature rise associated with joule heating in the metal. Because of the diffusion constant's strong temperature dependence, a modest 30 °C rise in the metal line temperature produces a corresponding value of α is 2.4×10^{-2}/min, whose magnitude is in reasonable agreement with the results seen in Fig. 4. Since the gold film test structure was fabricated on a polyimide dielectric, which is a good thermal insulator, such a temperature rise is feasible due to joule heating given the large current densities employed during EM stressing. Using Schafft's description[30] of the temperature distribution due to joule heating and the specifics of the geometry of our test structures, numerical simulations showed a temperature rise of comparable magnitude in the gold metal line, which provides support for this analysis.

IV. DISCUSSION AND CONCLUSIONS

In summary, a saturation behavior has been seen in resistance measurements during EM stressing in test structures employing thin gold films. A simple model has been described which explains the characteristic behavior. The model is based on recent theoretical results[7–9,24,26] and limited experimental results[11,23,36] which predict formation during EM stressing of an oscillating pattern of stress gradients in thin, narrow metal films. The stress gradients arise when the metal linewidth becomes comparable to the grain size and there exists nonuniformity in the polycrystalline structure producing clusters of small grains separated by sections of larger bamboo or near-bamboo grains. Differences in the metal diffusivities in the cluster and near-bamboo regions cause alternating metal ion accumulation and depletion at the interfaces between regions during EM stressing. Initial tensile stress in the metal thin film due to high temperature deposition contributes to EM damage by creating voids. Using parameters from the literature, the model predicts an order of magnitude for the rate constant α and the saturation parameter C that are consistent with the experimental results obtained. In addition, the model predicts a current density dependence for the saturation parameter C which is also seen experimentally.

While EM studies are typically performed at elevated temperatures, the results obtained here for thin gold films show EM can occur in reasonably short times near room temperature where most electrical stressing occurs in devices and circuits during normal operation. This is important for commercial development of III–V circuits since most heterojunction devices employ gold metallization for contacts and interconnects. In addition, semiconductor device self-heating and joule heating in the metal line will further accelerate the EM phenomena by raising the temperature.

Finally, the use of resistance measurements to study the early stages of electromigration can be beneficial in developing and testing strategies to minimize EM damage. For example, the results and model described here show that stress gradient generation can be used to counteract and limit ion migration due to EM before line failure occurs. This suggests that metal deposition conditions might be engineered,[25] such as deposition at low temperatures, to achieve a more desirable grain size and distribution or reduced tensile stress that can be used to control EM.

[1] A. Christou, in *Electromigration and Electronic Device Degradation*, edited by A. Christou (Wiley, New York, 1994), Chap. 1, p. 1.
[2] S. D. Mukherjee, *Reliability and Degradation: Semiconductor Devices and Circuits*, edited by M. J. Howes and D. V. Morgan (Wiley, New York, 1981), Chap. 1, p. 1.
[3] T. E. Kazior, H. Hieslmair, and R. C. Brooks, Mater. Res. Soc. Symp. Proc. **184**, 249 (1990).
[4] C. Canali, F. Chiussi, F. Fantini, L. Umena, and M. Vanzi, Electron. Lett. **23**, 364 (1987).
[5] D. P. Wilt, *Proceedings of the Sixth International Conference on InP and Related Materials* (IEEE, Piscataway, NJ, 1994), p. 296.
[6] T. Kwok and P. S. Ho, in *Diffusion Phenomena in Thin Films and Microelectronic Materials*, edited by D. Gupta and P. S. Ho (Noyes, Park Ridge, NJ, 1988), Chap. 7, p. 369.
[7] M. A. Korhonen, C. A. Paszkiet, and C. Y. Li, J. Appl. Phys. **69**, 8083 (1991).
[8] M. A. Korhonen, W. R. LaFontaine, P. Borgenson, and C. Y. Li, J. Appl. Phys. **70**, 6774 (1991).
[9] M. A. Korhonen, P. Borgenson, D. D. Brown, and C. Y. Li, J. Appl. Phys. **74**, 4995 (1993).
[10] P. F. Tang, A. G. Milnes, C. L. Bauer, and S. Mahajan, Mater. Res. Soc. Symp. Proc. **167**, 341 (1990).
[11] A. Scorzoni, B. Neri, and F. Fantini, Mater. Sci. Rep. **7**, 143 (1991).
[12] K. L. Tai and M. Ohring, J. Appl. Phys. **48**, 36 (1977).
[13] F. M. d'Heurle and P. S. Ho, in *Thin Films-Interdiffusion and Reactions*, edited by J. M. Poate, K. N. Tu, and J. W. Mayer (Wiley, New York, 1978), Chap. 8, p. 243.
[14] A. T. English, K. L. Tai, and P. A. Turner, J. Appl. Phys. **45**, 3757 (1974).
[15] H. M. Breitling and R. E. Hummel, J. Phys. Chem. Solids **33**, 845 (1972).
[16] R. E. Hummel, R. T. DeHoff, S. Matts-Goho, and W. M. Goho, Thin Solid Films **78**, 1 (1981).
[17] J. Y. Kim and R. E. Hummel, Phys. Status Solidi A **122**, 255 (1990).
[18] J. Y. Kim and R. E. Hummel, Phys. Status Solidi A **124**, 211 (1991).
[19] R. E. Hummel, B. K. Krumeich, and R. T. DeHoff, Appl. Phys. Lett. **33**, 960 (1978).
[20] J. Y. Kim, R. E. Hummel, and R. T. DeHoff, J. Vac. Sci. Technol. A **7**, 1273 (1989).
[21] S. Y. Lee, R. E. Hummel, and R. T. DeHoff, Thin Solid Films **149**, 29 (1987).
[22] G. L. Baldini and A. Scorzoni, IEEE Trans. Electron Devices **38**, 469 (1991).
[23] Z. Li, C. L. Bauer, S. Mahajan, and A. G. Milnes, J. Appl. Phys. **72**, 1821 (1992).
[24] B. D. Knowlton, J. J. Clement, and C. V. Thompson, J. Appl. Phys. **81**, 6073 (1997).
[25] L. He and Z. Q. Shi, Solid-State Electron. **39**, 1811 (1996).

[26] M. A. Korhonen, P. Borgenson, K. N. Tu, and C. Y. Li, J. Appl. Phys. **73**, 3790 (1993).
[27] C. Y. Li, P. Borgenson, and T. D. Sullivan, Appl. Phys. Lett. **59**, 1464 (1991).
[28] I. DeMunari, A. Scorzoni, F. Tamarri, D. Govoni, F. Corticelli, and F. Fantini, IEEE Trans. Electron Devices **41**, 2276 (1994).
[29] A. Scorzoni, I. DeMunari, and H. Stulens, Mater. Res. Soc. Symp. Proc. **337**, 515 (1994).
[30] H. A. Schafft, IEEE Trans. Electron Devices **34**, 664 (1987).
[31] K. N. Tu, Phys. Rev. B **45**, 1409 (1992).
[32] *CRC Handbook of Physics and Chemistry*, 73rd ed., edited by D. R. Lide (CRC, Boca Raton, FL, 1992) pp. 12–34.
[33] *ASM Metals Handbook*, 10th ed., edited by S. R. Lampman (ASM International, New York, 1990), p. 704.
[34] N. W. Ashcroft and N. D. Mermin, *Solid State Physics* (Holt, Rinehart and Winston, New York, 1976), p. 391.
[35] I. A. Blech and C. Herring, Appl. Phys. Lett. **29**, 131 (1976).
[36] E. Kinsbron, I. A. Blech, and Y. Komem, Thin Solid Films **46**, 139 (1977).